ELSEVIER

Earth and Planetary Science Letters 144 (1996) E9–E14

EPSL

Express Letter

Saw-toothed pattern of sedimentary paleointensity records explained by cumulative viscous remanence

Yvo S. Kok [a,*], Lisa Tauxe [a,b]

[a] *Fort Hoofddijk Paleomagnetic Laboratory, Budapestlaan 17, 3584 CD Utrecht, The Netherlands*
[b] *Scripps Institution of Oceanography, La Jolla, CA 92093-0220, USA*

Received 17 July 1996; accepted 30 August 1996

Abstract

The relative paleointensity of the earth's magnetic field from ODP Site 851 has been characterized by progressive decay towards polarity reversals, followed by sharp recovery of pre-reversal values [1]. We resampled the Gilbert–Gauβ reversal boundary of this deep-sea core, and show that during demagnetization this 'saw-toothed' pattern disappears. Further, the recently published Cumulative Viscous Remanence model [2] using the herewith obtained paleointensity record and constraints from thermal treatment replicates the saw-tooth of [1], implying that it is of non-geomagnetic origin.

Keywords: viscous remanent magnetization; paleomagnetism; Gilbert Epoch; Gauss Epoch; reversals; magnetic field

1. Introduction

Detrital remanence magnetism (DRM) of sediments is thought to be linearly related to the ambient field during deposition [3], hence accurate analyses of their magnetic characteristics could provide us with the long-term behavior of the geomagnetic field. To compensate for both contaminations as well as 'magnetizability' of the sedimentary rocks, several normalization techniques are available, using either division of the remanence after a certain demagnetization step by some bulk parameter (see review [4]), or the comparison of an interval of demagnetization treatments with the acquisition of remanence in the laboratory (see e.g. [5]). Several sedimentary paleointensity records of the earth's magnetic field show a distinct saw-toothed pattern (see e.g. [1,6,7]), in which a progressive decay of the field leading to reversals is followed by rapid post-reversal recovery. Supposing this observation to be a common characteristic of geomagnetic field behavior, severe implications on processes within the interior of our planet are imposed. Doubt was raised when a $^{10}Be/^{9}Be$ record across the youngest reversal indicated no offset in pre- and post-transitional geomagnetic field strengths [8]. Recently, we published an alternative explanation for the saw-toothed pattern, which explained the effect by a long-term Cumulative Viscous Remanence model (CVR) [2]. The saw-tooth has also been explained by a comparable model with delayed acquisition of the natural remanence (NRM) [9]. The purpose of our study is to re-analyze some of the deep-sea sediments used in the pioneer study by Valet and Meynadier [1]. Increased thermal and alternating field demagnetizations show that the

* Corresponding author. Fax: +31 30 253 5030. E-mail: yvoskok@geof.ruu.nl

PII S0012-821X(96)00175-6

saw-tooth disappears. Further, we show that the experimentally derived parameters for CVR are appropriate to explain the artificial nature of the saw-tooth.

2. Samples and methods

Valet and Meynadier constructed a paleointensity record for the last 4 million years by alternating field demagnetization to 15 or 20 mT of deep-sea sediments retrieved in the Eastern Equatorial Pacific during ODP Leg 138 [1]. In this study we will focus on the Gilbert–Gauß transition (3.6 Ma), which showed a substantial post-reversal recovery in [1]. Discrete samples in small glass tubes were taken from Holes 851B and E, drilled at 2°46′N, 110°34′W, and 3760 m water depth. The typical sampling strategy was ~ 1 cm^3 every ~ 3 cm. The depth–age model for Site 851 is that of [10]. We thermally demagnetized specimens of Hole 851E in the magnetically shielded room of Scripps Institution of Oceanography. The wet specimens were placed in elevated temperatures for 45 min from set point, followed by in situ cooling to room temperature enhanced by forced air. Partial thermal remanence (p-TRM) was induced by applying an axial field of 40.0 μT. This Thellier–Thellier type method has been shown to be successful for relative paleointensity estimates of ODP Leg 130 sediments [11].

Additional alternating field demagnetization of sediments from Hole 851B took place at Fort Hoofddijk. The acquisition of anhysteretic remanence (ARM) was imparted in a vertical field of 42 μT.

Total magnetic susceptibilities, χ, were measured on a Jelinek susceptibility bridge type KLY-2.02 before demagnetization. Thermomagnetic runs on the modified Curie balance [12] at Fort Hoofddijk indicated that alterations occur above 400°C, probably caused by magnetite formed through breakdown of sulfides.

3. Demagnetization results

Fig. 1 displays NRM directions and intensities of Hole 851E after demagnetization to various temperature steps normalized by total susceptibility. Before demagnetization, the Gauβ part of this normalized

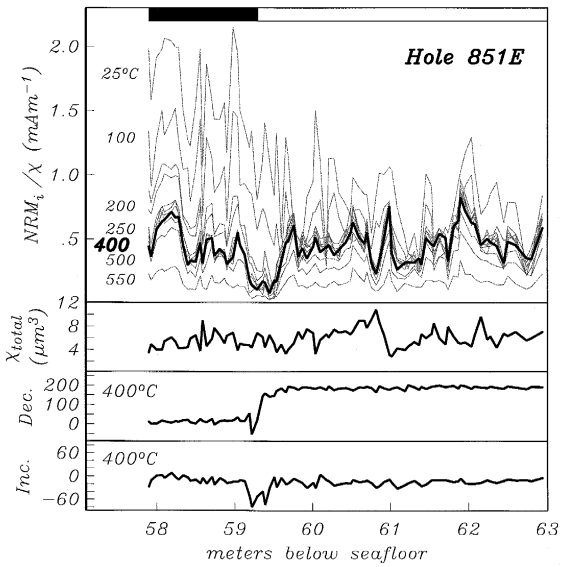

Fig. 1. NRM intensities of ODP 138-851E-7H after thermal demagnetization treatments (every 50°C starting at 100°C) normalized by χ. Low temperatures have not removed overprints and show post-transitional recovery above 59.3 m below seafloor (mbsf). From 250°C and up an 'even-shouldered' pattern around the transition is evident. The normalizer χ_{total} before thermal procedure and characteristic directions after demagnetization to 400°C are shown in lower panels. Polarities are depicted by black (Gauβ) and white (Gilbert) bars.

intensity record shows remarkably higher values than the Gilbert, producing the characteristic offset of the saw-tooth. The effect of increased temperature results in a dramatically greater decay in the post-transitional Gauβ than in the pre-transitional Gilbert. In the 250–400°C interval, the post-reversal jump towards higher values has disappeared entirely. Temperature treatments higher than 400°C should be viewed with caution, because of the possibility of alteration suggested by the thermomagnetic data. The normalizer χ_{total} (not weight corrected) is shown for completeness.

Alternating field demagnetizations were performed on samples of the parallel section Hole 851B. Fig. 2 shows the decay of the NRM intensities normalized by the anhysteretic remanence acquired at 100 mT alternating field (ARM_{max}). Like the thermal results, the intensity decay of the youngest part of the record is clearly larger. However, a minor offset after some 70 mT is still present and demagne-

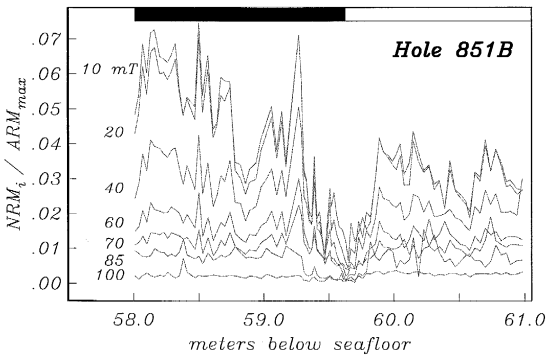

Fig. 2. Several NRM intensities of ODP 138-851B-7H after alternating field demagnetization treatments normalized by the ARM acquired at 100 mT. Low AF fields still indicate the offset of the saw-toothed pattern, whereas increased AF fields show a larger decay in the youngest part (above 59.6 mbsf). However, a reliable symmetric pattern around the transition is not established. Polarities as in Fig. 1.

tizations to higher AF fields give rise to unstable intensities and directions. Since the offset disappears completely on thermal cleaning, we assume the alternating field demagnetizations to be of lower fidelity, also, there the mechanism of AF demagnetization is never fully understood. Moreover, it will not provide constraints for our thermal activation model.

4. Alternative explanations for the saw-tooth

A model calling on long-term cumulative viscous effects of the magnetic remanence gives an alternative explanation for the saw-toothed patterns in paleointensity records [2]. We have argued that the initial detrital magnetization after deposition, M_o, is not in

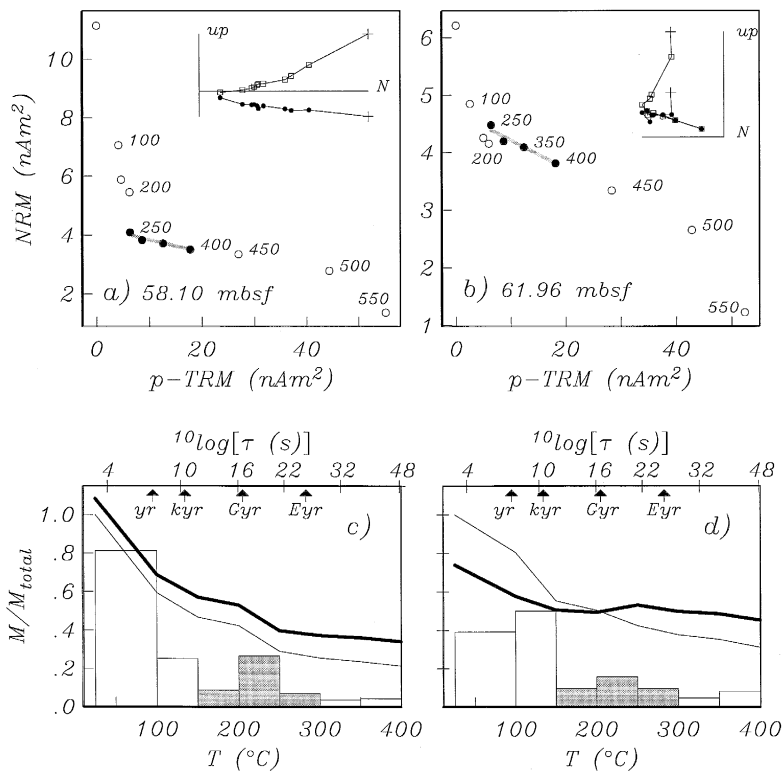

Fig. 3. Typical results for thermal demagnetization and acquisition from Hole 851E for a Gauβ sample (left), and a Gilbert sample (right). (a) and (b) Arai plots indicate segmented line (see text). Insets represent Zijderveld diagrams of stepwise thermal demagnetizations. (c) and (d) The decay curves as function of temperature for the intensity (heavy line) and for the sum of the norms of the vector differences intensity (thin) tied to 550°C. The unblocking spectra of the latter are indicated by bins. Conversion from unblocking temperature to relaxation times, τ, at the ocean floor ($T = 2$°C) results in upper logarithmic scale (see text). Shaded areas indicate the unblocking of particles argued to give rise to long-term viscous effects.

equilibrium with the external earth magnetic field, inducing a relaxation process towards an unknown equilibrium remanence, M_e. The rate of the growth is not only controlled by the relaxation time, τ, but also by the degree to which the initial magnetization is out of equilibrium. Since its deposition the sample has witnessed varying paleofields with either parallel or anti-parallel polarities, which could have significant consequences for the evolution of the total remanence. We calculate the cumulative magnetization at present after $(n-1)$ polarity reversals, as the last term (M_n) of the sequence:

$$M_k = \left\{ (-1)^{k+1} M_e + \frac{M_{k-1} + (-1)^k M_e}{N} \times \sum_{i=1}^{N} e^{-\Delta t_k / \tau i} \right\}_{k=1}^{n} \quad (1)$$

where the term M_k is the magnetization acquired during the kth polarity interval with duration Δt_k, and N the number of values τ_i. The Cumulative Viscous Remanence model (CVR) used $M_o = 1$ (arbitrary unit), typical values between 5 and 100 Myr for $f(\tau)$ and 5 and 30 for the constant M_e [2].

Another alternative explanation for the saw-tooth in paleointensity records is given by Mazaud [9]. Again, a softer magnetic component is acquired after deposition. A large fraction (X) of the magnetic grains acquires NRM at the time of deposition, while the remaining grains reorientate or acquire magnetization after deposition. The difference between the two alternatives is that, in the latter model, the secondary magnetization is locked in physically, whereas in the former it always relaxes to the varying equilibrium magnetizations. It is difficult to obtain experimental constraints for the parameters X and lock-in time. On the other hand, we are able to constrain M_e and the distribution of relaxation times $f(\tau)$ existing in the specimen using thermal experiments.

4.1. Equilibrium magnetization M_e

We suspect an induced thermal remanence (TRM) will be in equilibrium with the applied field, and would be an estimate for M_e. Because of the alteration of the samples above 400°C, we cannot simply impart a total TRM to determine the value of M_e. For this reason, we subjected each specimen to a Thellier–Thellier type experiment [11,13]. Zijderveld diagrams of thermal demagnetization of a Gauβ and a Gilbert specimen are shown in the insets of Fig. 3a and b, respectively. After circa 250°C a soft component has been removed and more or less stable vectors are encountered (see also Fig. 1). The Arai plots [14] of NRM remaining versus p-TRM acquired show distinct segments: (1) a soft interval up to 250°C; (2) a more stable segment from 250 to 400°C; and (3) the higher temperature steps that were expected have suffered from magnetic alterations, although intensities of both NRM and TRM do not appear to be wildly deviant even up to 500°C. The slopes of the middle segment vary from -0.02 to -0.10; in other words, the p-TRM acquisition is 10–50 times more efficient than the DRM. This range is the effect of the paleofield variations ($\pm 60\%$) around a certain mean. If the average ancient field was equal to the laboratory field (40.0 μT), M_e would be constrained to be the mean of this range of approximately 30 (i.e. ~ 30 times more efficient than $M_o = 1$). Naturally, we do not know the ancient field strength. However, Constable and Tauxe [15] provide a possible means for a quantative calibration. They suggest that if: (1) the axial dipole term is assumed zero at the midpoint of the transition and (2) the average non-axial dipole field is assumed to have the present-day average value of 7.5 μT everywhere, then the relative intensity records can be transformed into quasi-absolute values. In this way, the non-transitional average paleofield intensity for our Gilbert–Gauβ data is 32 μT. It is noteworthy that the IGRF value at Site 851 is also 32 μT. Presuming linearity, an estimate for the equilibrium magnetization is $M_e = (32/40) \times \sim 30 = \sim 24$.

4.2. Relaxation times τ_i

In Fig. 3c,d, the intensity decay data of the samples shown in Fig. 3a,b are plotted as a heavy line. Also shown is the sum of the norms of the vector differences, which takes care of anti-parallel directions (thin line). The unblocking spectrum of this monotonic decay is plotted as a function of temperature on the lower horizontal axis. In our thermal

demagnetization experiment, the specimen must have been exposed to temperature T_{lab} for at least some 5 min ($t_{ub} = 300$ s). If the magnetization has unblocked to 5% of its initial value (i.e., $e^{-t_{ub}/\tau_{lab}} = 0.05$), then the unblocking time, t_{ub}, will be 3 times the 'effective' relaxation time in the laboratory, τ_{lab}. Therefore, we estimate this relaxation time in our thermal experiments to be 100 s. Following Pullaiah et al. [16], we assume that the coercivity of the magnetic grains is shape dominated; hence, $H_c(T)$ is proportional to $J_s(T)$. By rearranging their equation 2 we obtain:

$$\ln(C\tau_{ocean}) = \frac{T_{lab}}{T_{ocean}} \frac{\ln(C\tau_{lab})}{J_s^2(T_{lab})} \qquad (2)$$

where C is the characteristic frequency of thermal fluctuation ($\sim 10^{10}$ Hz); T_{ocean} the temperature at the ocean floor (2°C = 275 K); and $J_s(T)$ the spontaneous magnetization as function of temperature of Ward's standard magnetite (data courtesy J. Gee), assuming $J_s\ (T_{ocean}) = 1$ (arbitrary unit). By using Eq. (2), the laboratory-induced unblocking temperatures are converted to relaxation times under ocean floor conditions on the logarithmic upper scale in Fig. 3c,d. For example, at $T_{lab} = 200$°C, Eq. (2) reduces to $\tau_{ocean} = C^{1.17} \times \tau_{lab}^{2.17}$. Using $\tau_{lab} = 100$ s, one obtains a τ_{ocean} of circa 350 Myr ($\sim 10^{16}$ s). Small variations in the adopted τ_{lab} have no drastic influence on the calculation, keeping in mind that the exposure time at the ocean floor is two orders of magnitude shorter (10^{14} s, ~ 3.5 Myr) than τ_{ocean}.

The large peaks in the unblocking spectra at low temperatures indicate the unblocking of those particles that contribute only to the short-term viscous effects (10^8 s, ~ 3 yr). We suppose that the long-term viscous effects are caused by grains that are unblocked in the secondary peak (150–300°C, shaded intervals, Fig. 3c,d), implying that the mean of the relaxation time distribution τ_i will be between 10^{16} s (~ 200°C) and 10^{22} s (~ 250°C).

It appears that the logarithm of the distribution of relaxation times is consistent with a Gauβ–Laplace distribution with a mean of circa 16.5 and standard deviation of 5.5; that is, $f(\tau) = 10^{16.5 \pm 5.5}$ s. At $T_{lab} = 400$°C, grains with astronomical τ_{ocean} values of 10^{48} s are unblocked; these will not contribute to the CVR in a few million years and presumably carry the 'stable' magnetic information. To exclude as many viscously behaving components as possible from the usual paleointensity calculation (slope of the stable 250–400°C interval in the Arai plot), we use only the 400°C step for the paleointensity estimates.

5. Remodeling the saw-tooth

For simplicity, we assumed a constant initial remanence $M_o = 1$ in our first modeling attempts [2]. If one interprets the NRM_{400}/χ record as representing the real paleointensity fluctuations, it can be used as input for the described CVR model (normalized by the mean of the record). Together with its experimentally constrained parameters $f(\tau)$ and M_e, it results in the NRM at present as plotted in Fig. 4. The grey curve represents the alleged paleointensity (NRM_{400}/χ), the heavy line is the calculated NRM at present (CVR), which agrees remarkably well with the thin Valet and Meynadier curve [1] (VM93).

Dating discrepancies between CVR and VM93 stem from the ambiguous conversion and interpolations from meters below sea floor (Hole 851E) via meters composite depth (Site 851) to depositional age [10]. Small amplitude differences can be explained by the fact that we characterized our 5 m record by a constant set of parameters. We note that

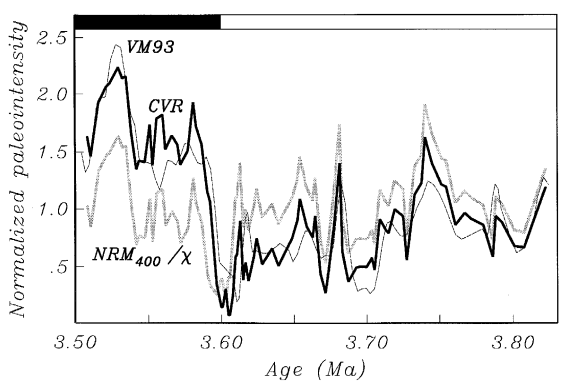

Fig. 4. Paleointensity records normalized by their means as function of depositional age. Grey line represents the NRM_{400}/χ paleointensities fed to the Cumulative Viscous Remanence model with parameters $M_e = 24$ and $\tau_i = 10^{16.5 \pm 5.5}$ s ($N = 1000$), resulting in CVR curve. Also shown are typical 'saw-toothed' data (20 mT alternating field demagnetization) from the same site normalized by their mean value by Valet and Meynadier (VM93). The CVR displays strong similarities with VM93, supporting the artificial origin of saw-toothed patterns in paleointensity records.

the corresponding finer scale features appear in all records, wholly contradicting the rationalization that VRM would erase or obscure these properties [7].

6. Conclusion

The occasionally detected saw-toothed pattern in sedimentary relative paleointensity records (see e.g. [1,6,7]) can be explained by unremoved remanence acquired since deposition. Thermal demagnetization of the re-examined Gilbert–Gauβ reversal causes the large post-transitional recovery of the paleofield intensity to disappear entirely. Using our NRM_{400}/χ paleointensity estimates as well as model parameters derived from Thellier–Thellier type experiments, the Cumulative Viscous Remanence model [2] calculates an NRM at present that is virtually identical with previous results of Valet and Meynadier. Thus, the likelihood that the contamination is of long-term viscous origin is considerable.

Acknowledgements

We thank Paul Hartl, Bryan Conlon, Cor de Boer, and ODP personnel at College Station for help in the laboratory, Jeff Gee for Ward's magnetite data, and — of course — Chet Baker. Comments and suggestions by Cor Langereis, Mark Dekkers, Harmen 'doctor' Bijwaard, Cathy Constable, and two anonymous referees helped to improve the manuscript. The investigations were supported by the Netherlands Geosciences Foundation (GOA) with financial aid from the Netherlands Organization for Scientific Research (NWO) (750.194.09). Further financial support by National Science Foundation (NSF). ***[RV]***

References

[1] J.-P. Valet and L. Meynadier, Geomagnetic field intensity and reversals during the past four million years, Nature 366, 234–238, 1993.

[2] Y.S. Kok and L. Tauxe, Saw-toothed paftern of relative paleointensity records and cumulative viscous remanence, Earth Planet. Sci. Lett. 137, 95–99, 1996.

[3] D.V. Kent, Post-depositional remanent magnetisation in deep-sea sediment, Nature 246, 32–34, 1973.

[4] L. Tauxe, Sedimentary records of relative paleointensity of the geomagnetic field in sediments: theory and practice. Rev. Geophys., 31, 319–354, 1993.

[5] L. Tauxe, T. Pick and Y.S. Kok, Relative paleointensity in sediments; a pseudo-Thellier approach, Geophys. Res. Lett. 22, 2885–2888, 1995.

[6] J.-P. Valet, L. Meynadier, F.C. Bassinot and Fl. Garnier, Relative paleointensity across the last geomagnetic reversal from sediments of the Atlantic, Indian and Pacific oceans, Geophys. Res. Lett. 21, 485–488, 1994.

[7] K.L. Verosub, E. Herrero-Bervera and A.P. Roberts, Relative geomagnetic paleointensity across the Jaramillo subchron and the Matuyama/Brunhes boundary, Geophys. Res. Lett. 23, 467–470, 1996.

[8] G.M. Raisbeck, F. Yiou and S.Z. Zhou, Paleointensity puzzle, Nature 371, 207–208, 1994.

[9] A. Mazaud, 'Sawtooth' variation in magnetic intensity profiles and delayed acquisition of magnetization in deep sea cores, Earth Planet. Sci. Lett. 139, 379–386, 1996.

[10] N.J. Shackleton, S. Crowhurst, T. Hagelberg, N.G. Pisias and D.A. Schneider, A new Late Neogene time scale: application to Leg 138 Sites, Proc. ODP Sci. Results 138, 73–101, 1995.

[11] P. Hartl and L. Tauxe, A precursor to the Matuyama/Brunhes transition-field instability as recorded in pelagic sediments, Earth Planet. Sci. Lett. 138, 121–135, 1996.

[12] T.A.T. Mullender, A.J. Van Velzen and M.J. Dekkers, Continuous drift correction and separate identification of ferrimagnetic and paramagnetic contributions in thermomagnetic runs, Geophys. J. Int. 114, 663–672, 1993.

[13] E. Thellier and O. Thellier, Sur l'intensité du damp magnétique terrestre dans le passé historique et géologique, Ann. Geophys. 15, 285–378, 1959.

[14] T. Nagata, Y. Arai and K. Momose, Secular variation of the geomagnetic total force during the last 5000 years, J. Geophys. Res. 68, 5277–5282, 1963.

[15] C. Constable and L. Tauxe, Towards absolute calibration of sedimentary paleointensity records, Earth Planet. Sci. Lett. 143, 269–274, 1996.

[16] G. Pullaiah, E. Irving, K.L. Buchan and D.J. Dunlop, Magnetization changes caused by burial and uplift, Earth Planet. Sci. Lett. 28, 133–143, 1975.